AIAA JOURNAL
Vol. 30, No. 4, April 1992

Pressure Drop in Fully Developed, Turbulent, Liquid-Vapor Annular Flows in Zero Gravity

K. R. Sridhar*
University of Arizona, Tucson, Arizona 85721
and
B. T. Chao† and S. L. Soo‡
University of Illinois, Urbana, Illinois 61801

The prediction of frictional pressure drop in fully developed, turbulent, *annular* liquid-vapor flows in zero gravity using simulation experiments conducted on Earth is described. The scheme extends the authors' earlier work on *dispersed* flows. The simulation experiments used two immiscible liquids of identical density, namely, water and n-butyl benzoate. Because of the lack of rigorous analytical models for turbulent, annular flows, the proposed scheme resorts to existing semiempirical correlations. Results based on two different correlations are presented and compared. Others may be used. It was shown that, for both *dispersed* and *annular* flow regimes, the predicted frictional pressure gradients in 0-*g* are lower than those in 1-*g* under otherwise identical conditions. The physical basis for this finding is given.

I. Introduction and Background

In recent years, there has been renewed interest in the dynamics and thermodynamics of liquid-vapor flows in micro- and reduced gravity. This interest stems from the anticipation that spacecrafts, platforms, and space bases of the future will require thermal control systems with design requirements far more complex than those currently in use. It is envisioned that such systems will employ two-phase flow media, because boiling and condensation offer the advantages of near isothermality of operation, high heat transfer rates, and, hence, significant weight reduction. The subject is also of interest in the area of extraterrestrial materials extraction and processing. Among other things, the design of such thermal control systems would require information on pumping power requirements, and, hence, the need for the prediction of two-phase frictional pressure drop in duct flow under micro- and reduced gravity conditions.

A survey of literature on liquid-vapor flows in zero and reduced gravity was presented by Sridhar et al.[1] An ideal laboratory to conduct studies in 0-*g* would be aboard a space station or an orbiting space vehicle such as the Space Shuttle. However, the availability of a space station is many years away, and the cost of conducting liquid-vapor flow experiments in the shuttle is prohibitively high, and its accessibility is limited. An alternative is to develop Earth-based techniques for simulating a 0-*g* environment. Earth-based testing can, in some cases, eliminate the need for conducting experiments in zero and reduced gravity and, in others, provide partial answers, thereby reducing the time and cost involved in the design of new systems. Several techniques of creating zero and reduced gravity effects have been used in the past. A detailed discussion of these techniques and their limitations can be found in Sridhar.[2]

Important design parameters such as frictional pressure drop and heat transfer coefficients for liquid-vapor flows depend greatly on the flow regime. Hence, knowledge of flow regimes that would exist in microgravity environments is important. Some of the flow regime studies were based on analytically extrapolating the existing 1-*g* flow regime maps to microgravity conditions.[3,4] Others were based on liquid-vapor experiments conducted aboard aircraft flying parabolic trajectories.[5,6] While reliable microgravity flow regime maps are yet to be developed, all investigators seem to agree on the existence of three flow regimes, viz., dispersed, intermittent, and annular or annular mist. A method of determining the frictional pressure drop in fully developed duct flow of *dispersed* liquid-vapor mixture at zero gravity has been proposed by the authors.[1] This paper concerns the *annular* regime.

The dynamics of annular two-phase flow is complex and, at the present time, rigorous analytical models do not exist. The complexity arises from, among other things, the existence of many varieties of interfacial configurations that are dependent upon the flow velocities, flow geometries, and the bulk and interfacial properties of the phases. In annular flows, a central problem is to determine the interrelationship among film flow rate, effective film thickness, and pressure gradient. At the present time, this so-called triangular relationship cannot be derived from first principles. However, a number of empirical correlations that relate two of the three variables are available. One class of such correlations is based on the premise that the amplitude of the interfacial waves will increase with increasing film thickness and that the roughness of the interface is independent of the gas flow rate. In this class of correlations, the friction factor is usually related to a dimensionless film thickness expressed as the ratio of film height to pipe diameter. An early attempt was that of Calvert and Williams in 1955,[7] and it has since been used by many others.[8-15] A brief review of these correlations can be found in Hewitt and Hall-Taylor.[16]

Henstock and Hanratty[17] conducted air-water experiments for vertical flows in 31.4 mm and 34.5 mm pipes and proposed correlations between the ratio of the interfacial friction factor to the single-phase flow wall friction factor and the ratio of the film height to the pipe diameter for upflow, downflow, and horizontal flows. Asali et al.[18] conducted experiments for vertical flows of air and water and for air and water-glycerine solutions in pipes of different diameters. Analysis of their own data and earlier data reported by Cousins et al.[19] and by Shearer and Nedderman,[13] as well as vertical downflow data by Andreussi and Zanelli[20] and by Webb,[21] led them to con-

Received June 11, 1991; accepted for publication July 26, 1991.

*Assistant Professor, Department of Aerospace and Mechanical Engineering. Member AIAA.
†Professor Emeritus, Department of Mechanical and Industrial Engineering.
‡Professor, Department of Mechanical and Industrial Engineering.

clude that the friction factor ratio could be better correlated with a film thickness made dimensionless with a gas phase friction length.

Recently, Klausner[22] performed extensive pressure drop measurements for vapor-liquid annular flow of refrigerant R11 in a 19.1 mm tube, vertically upward and downward, as well as horizontal. Although Klausner's upflow data can be reasonably well correlated by Asali et al.'s scheme,[18] it is not possible to collapse the downflow data, particularly when the film height is not small. Thus, from our review of the literature, it can be said that friction factor correlations of general validity have yet to be determined. The purpose of the present study is to demonstrate how the two-phase frictional pressure drop in fully developed *annular* duct flow under zero gravity may be predicted by using simulation experiments conducted in an Earth-based facility. The simulation scheme employs two immiscible, neutrally buoyant liquids, and the friction factor correlations used were those of Henstock and Hanratty[17] and of Asali et al.[18] Results based on these two different correlations are compared and discussed. The predicted 0-g pressure drops are also compared to Earth-gravity predictions. It should be noted that the proposed scheme is not limited to the two correlations cited. Others of more general validity should obviously be used when they become available.

II. Theoretical Basis of Simulation for Steady, Fully Developed Annular Flows in Straight Conduits

Figure 1 depicts the geometry of two-phase annular flow in a circular pipe of inner radius r_0 (which is also the outer radius of the annular film) with its axis z inclined at an angle θ with the upward vertical axis ζ. The ζ axis is colinear with the local gravitational vector $\bar{g}$, but in the *opposite* direction. The analysis presented here is one dimensional and for fully developed flow without entrainment. Denoting the mean inner radius of the annular film by r_i, material density by ρ, interfacial shear stress by τ_i, shear stress at the pipe wall by τ_w, and static pressure by P, and using the subscript F for the annular film and C for the core fluid, the steady-state momentum equation for the fully developed annular film flow is

$$-(r_0^2 - r_i^2)\frac{dP}{dz} - 2r_0\tau_w + 2r_i\tau_i - \rho_F g(r_0^2 - r_i^2)\cos\theta = 0 \quad (1)$$

and that for the core fluid is

$$-r_i^2\frac{dP}{dz} - 2r_i\tau_i - \rho_C g r_i^2\cos\theta = 0 \quad (2)$$

Equivalent forms of (1) and (2) are

$$-\frac{dP}{dz} = 2\tau_w\frac{r_0}{r_0^2 - r_i^2} - 2\tau_i\frac{r_i}{r_0^2 - r_i^2} + \rho_F g\cos\theta \quad (3)$$

and

$$-\frac{dP}{dz} = 2\tau_i\frac{1}{r_i} + \rho_C g\cos\theta \quad (4)$$

Eliminating dP/dz from Eqs. (3) and (4) gives

$$\frac{2r_0^2}{r_0^2 - r_i^2}\left(\frac{\tau_w}{r_0} - \frac{\tau_i}{r_i}\right) + (\rho_F - \rho_C)g\cos\theta = 0 \quad (5)$$

For liquid-vapor flows in zero gravity, Eq. (5) becomes

$$\frac{\tau_i}{\tau_w} = \frac{r_i}{r_0} \quad (6)$$

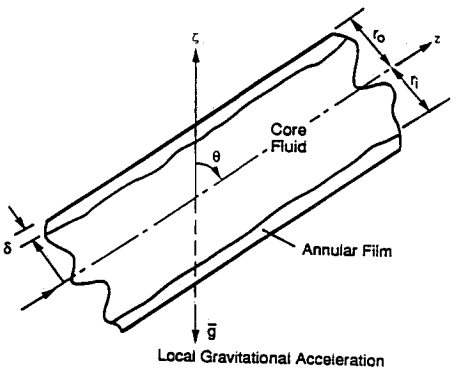

Fig. 1 Fully developed annular flow in a straight conduit.

and the pressure gradient is the frictional pressure gradient. It is given by

$$-\left(\frac{dP}{dz}\right)_f = \frac{2\tau_i}{r_i} \quad (7)$$

where the subscript f refers to friction.

For the simulation experiments on Earth using horizontal flows, Eqs. (6) and (7) remain valid because $\rho_F = \rho_C$ and $\cos\theta = 0$. The static pressure gradient is also the frictional pressure gradient. We note that Eqs. (6) and (7) will not hold by simply selecting $\cos\theta = 0$ (horizontal flow) without requiring $\rho_F = \rho_C$ because stratification would occur when $\rho_F \neq \rho_C$ and the assumed annular flow could not be realized. This observation does not follow from the equations just cited because of the one-dimensional assumption used.

We now digress and compare the simulation scheme for *dispersed* two-phase flows[1] with that used in the present study. It was demonstrated by Sridhar et al.[1] that for steady, fully developed *dispersed* flows in straight conduits of constant cross section the dispersed and continuous phase velocities are equal for liquid-vapor flows in 0-g and for neutrally buoyant flows in 1-g. The pressure drop in liquid-vapor flow in 0-g is identical to that due to liquid flowing alone at the same combined volumetric flow rate and, thus, can be readily determined. For annular flows, the situation is more complex, even for the ideal case of no entrainment. Equation (6) or (7) provides no information on the flow properties of interest, namely, the interfacial shear stress and the film thickness or the volume fraction of the annular fluid. Unfortunately, rigorously derived equations are not available for their prediction at the present time. One has to resort to correlations available in the literature. Without exception, the correlations are based on experimental data and invariably involve some empiricism. Furthermore, they are not universally valid. In the words of Hewitt,[23] "Over the past 30 years, continuing attempts have been made to derive better correlations for frictional pressure gradient. As more data became available, the deficiencies of earlier correlations became apparent and further correlations were developed. This process is a continuing one, and it reflects the fact that, for a situation as complex as two-phase flow, it is very difficult to formulate relationships that have a general physical basis." (pp. 2–58 and 2–59). For this reason, two different correlations were used in the present study, and the simulation results were compared. Details follow.

A. Simulation Based on Asali et al. Correlation [18]

Asali et al.[18] conducted vertical annular upflow experiments with air as the core fluid and water and water-glycerine solutions as the film fluid in straight circular pipes with inside diameter of 22.9 mm and 42.0 mm. The viscosity of the film fluid varied from 1.1 mPa·s to 5.0 mPa·s. Average film thickness, film flow rate, and pressure drop were measured. They observed that at low liquid flow rates the film was smooth

except for interspersed long, crested ripples, which they described as ripple waves. At high liquid flow rates, coherent roll waves, which moved at much higher velocities than the ripples, appeared on the film. The transition was accompanied by an atomization of the liquid at the wave crest. Separate correlations were given for the frictional pressure drop in the two regimes. For this study, the correlations for the ripple-wave regime are appropriate. The following is a brief recapitulation of the essence of the analysis and its results.

Denoting the mass flow rate by $\dot{M}$ and the dynamic viscosity by μ, the superficial film and core Reynolds numbers are

$$Re_F = \frac{2\dot{M}_F}{\pi r_0 \mu_F} \tag{8a}$$

and

$$Re_C = \frac{2\dot{M}_C}{\pi r_0 \mu_C} \tag{8b}$$

A friction factor f_i based on the interfacial shear is defined by

$$f_i = \frac{\tau_i}{(1/2)\rho_C U_C^2} \tag{9}$$

where U_C is the superficial velocity of the core fluid, $\dot{M}_C/(\pi r_0^2 \rho_C)$, and τ_i is related to the measured total pressure gradient according to

$$\tau_i = -\frac{dP}{dz}\left(\frac{r_0 - \delta}{2}\right) \tag{10}$$

in which δ is the average film thickness. The shortcoming of defining τ_i in terms of the total pressure gradient instead of its frictional component has been pointed out by Klausner.[22] However, in fully developed horizontal flows on Earth and fully developed flows in 0-g, the two pressure gradients become identical. For correlation purposes, f_i is related to f_s, which is the single-phase friction factor that would have existed in a smooth pipe if the core fluid filled the entire pipe, and they used $f_s = 0.046\, Re_C^{-0.20}$. A dimensionless film thickness m_g^+ based on the friction velocity associated with the core fluid is introduced. It is

$$m_g^+ = \delta(\tau_i/\rho_C)^{0.5}/\nu_C \tag{11}$$

where ν is the kinematic viscosity. Asali et al. gave the following correlations for the ripple wave regime.

For vertical upflows

$$\frac{f_i}{f_s} - 1 = C_1(m_g^+ - 4) \tag{12}$$

and

$$m_g^+ = 0.34\, Re_F^{0.6}\, \frac{\nu_F}{\nu_C}\left(\frac{\rho_F}{\rho_C}\frac{\tau_i}{\tau_{ch}}\right)^{0.5} \tag{13}$$

where τ_{ch} is the characteristic shear stress defined by $\tau_{ch} = 2/3\ \tau_w + 1/3\ \tau_i$ and τ_w is the wall shear stress.

For vertical downflows

$$\frac{f_i}{f_s} - 1 = C_2(m_g^+ - 5.9) \tag{14}$$

The downflow data used were those of Andreussi and Zanelli[20] and of Webb.[21] For core fluid velocities greater than 25 ms^{-1}, $C_1 = C_2 = 0.045$ and $\tau_i/\tau_{ch} \cong 1$. For lower core fluid velocities, $C_1 > 0.045$ and $C_2 < 0.045$. The numerical constants 4 and 5.9 in Eqs. (12) and (14) are to account for a critical film thickness below which the interface may be considered smooth. Equations (12) and (14) indicate that the form of the correlations for vertical upflow and downflow is essentially the same. Hence, one may argue that the same form can be used for horizontal flow as long as the flow is annular. Accordingly, for horizontal flows with thin annular films ($\tau_i/\tau_{ch} \cong 1$) and with sufficiently large core velocities, as is the case for the present investigation, we may write

$$\frac{f_i}{f_s} - 1 = K_1(m_g^+ - K_2) \tag{15}$$

and:

$$m_g^+ = K_3 Re_F^{K_4}\left(\frac{\mu_F}{\mu_C}\right)\left(\frac{\rho_C}{\rho_F}\right)^{0.5} \tag{16}$$

where K represents numerical constants. The data of Asali et al.[18] and others suggest that gravity, fluid properties, and pipe diameters would have no significant effect on K_1, K_3, and K_4, at least within the range of their experimental conditions. On the other hand, gravity may exert its influence on K_2. Also, when the core fluid velocities are below 25 ms^{-1}, K_1 may be dependent on gravity.

Combining Eqs. (15) and (16) gives

$$\frac{f_i}{f_s} - 1 = K_5 Re_F^{K_4} B - K_6 \tag{17}$$

where $K_5 = K_1K_3$, $K_6 = K_1K_2$, and $B = (\mu_F/\mu_C)(\rho_C/\rho_F)^{0.5}$. Now, the dynamics of fully developed, vertical annular liquid-vapor flows in a straight conduit in zero gravity should differ little from that of the same fluids in a horizontal flow of the same mass flow rates on Earth provided that the annular flow configuration can be obtained. Annular horizontal flow was indeed found to be possible on Earth in the neutrally buoyant, water-benzoate system, and the simulation scheme is based on the premise that Eq. (17) holds for annular liquid-vapor flow in 0-g, as well as for *horizontal*, annular water-benzoate flow on Earth. The values of the constants K_4, K_5, and K_6 are to be determined by conducting experiments in the water-benzoate system and using measured frictional pressure gradient for various combinations of Re_F and Re_C. As we shall demonstrate shortly, K_4, K_5, and K_6 are indeed constants, at least for the range of operating conditions employed in the present investigation.

B. Simulation Based on Henstock and Hanratty Correlation [17]

Henstock and Hanratty[17] developed a correlation for f_i/f_s that differs from that proposed by Asali et al.[18] The correlation was based mainly on the results of vertical air-water upflows in 31.4 mm and 34.5 mm i.d. pipes. A flow parameter F analogous to the Martinelli flow parameter was introduced. It is defined by

$$F = \frac{\phi(Re_F)}{Re_C^{0.9}}\left(\frac{\mu_F}{\mu_C}\right)\left(\frac{\rho_C}{\rho_F}\right)^{0.5} \tag{18}$$

where Re_F and Re_C are given by Eqs. (8a) and (8b), and the function $\phi(Re_F)$ is a dimensionless film thickness defined by

$$\phi(Re_F) = \delta(\tau_{ch}/\rho_F)^{0.5}/\nu_F \tag{19}$$

in which $\tau_{ch} = 2/3\ \tau_w + 1/3\ \tau_i$. Thus, the film thickness was made dimensionless by a length scale based on properties of the liquid film, in contrast to those of the vapor core used by Asali et al. The flow parameter F characterizes the "rough-

ness" of the interface. For thin films, $\tau_{ch} \cong \tau_i \cong \tau_w$, and Henstock and Hanratty gave

$$\phi(Re_F) = [(0.707\ Re_F^{0.5})^{2.5} + (0.0379\ Re_F^{0.9})^{2.5}]^{0.4} \quad (20)$$

The friction factor correlations are as follows.

For vertical upflows

$$\frac{f_i}{f_s} = 1 + 1400\ F \quad (21)$$

with $f_s = 0.046\ Re_C^{-0.20}$, the same as in Asali et al. correlation.

For vertical downflows

$$\frac{f_i}{f_s} = 1 + 1400\ K_C F \quad (22)$$

where the correction factor K_C accounts for gravity and is given by

$$K_C = 1 - \exp[-\tau_i/\rho_F \delta g] \quad (23)$$

The dimensionless parameter $(\tau_i/\rho_F \delta g)$ denotes the ratio of the shear force at the interface to the gravitational force. If Eq. (23) remains valid for microgravity, then $K_C \to 1$ as $g \to 0$. Thus, in 0-g, Eq. (21) holds for both upflows and downflows, as one would expect.

For convenience of further discussions, the properties associated with the film and the core fluid of the liquid-vapor system in 0-g and of the water-benzoate system in 1-g will be designated by subscripts as listed below:

	Liquid-Vapor Flow in 0-g	Water-Benzoate Flow in 1-g
Film Fluid (F)	L (liquid)	B (benzoate)
Core Fluid (C)	G (vapor)	W (water)

In the proposed simulation scheme, the correlation parameter F is chosen to be identical for the two systems in order to lessen the impact of the known shortcomings of the Henstock-Hanratty correlation.[17] We return to this point later. Accordingly, for equal F's of the two systems, we have

$$\frac{\phi(Re_L)}{Re_G^{0.9}} \frac{\mu_L}{\mu_G} \left(\frac{\rho_G}{\rho_L}\right)^{0.5} = \frac{\phi(Re_B)}{Re_W^{0.9}} \frac{\mu_B}{\mu_W} \quad (24)$$

Using the correlation given by Eq. (20), Eq. (24) can be recast into the following form:

$$\left[\frac{(0.707\ Re_B^{0.5})^{2.5} + (0.0379\ Re_B^{0.9})^{2.5}}{(0.707\ Re_L^{0.5})^{2.5} + (0.0379\ Re_L^{0.9})^{2.5}}\right]^{0.4} \left(\frac{Re_G}{Re_W}\right)^{0.9} = \frac{\mu_L}{\mu_G} \frac{\mu_W}{\mu_B} \left(\frac{\rho_G}{\rho_L}\right)^{0.5} \quad (25)$$

At room temperature, $\mu_W/\mu_B = 0.286$, and, thus, the right-hand side of Eq. (25) is completely determined from the property values of the liquid-vapor system of interest. Furthermore, for a given total mass flow rate and quality of the liquid-vapor flow in the duct, the superficial Reynolds numbers Re_G and Re_L are known. Either Re_W or Re_B can be chosen, and the other can be determined from Eq. (25).

The ratio of the frictional pressure gradients in the two systems is given by

$$\frac{\left(\frac{dP}{dz}\right)_{f(G/L)}}{\left(\frac{dP}{dz}\right)_{f(W/B)}} = \left[\frac{\tau_i(G/L)}{\tau_i(W/B)}\right] \cdot \left[\frac{r_i(W/B)}{r_i(G/L)}\right] = \frac{f_i(G/L)}{f_i(W/B)} \cdot \frac{\rho_G U_G^2}{\rho_W U_W^2} \cdot \frac{r_i(W/B)}{r_i(G/L)} \quad (26)$$

With identical F for both systems, the ratio of f_i for the two systems becomes identical to the ratio of f_s, and, hence, Eq. (26) becomes

$$\frac{\left(\frac{dP}{dz}\right)_{f(G/L)}}{\left(\frac{dP}{dz}\right)_{f(W/B)}} = \left(\frac{Re_G}{Re_W}\right)^{1.8} \left(\frac{\mu_G}{\mu_W}\right)^2 \cdot \frac{\rho_W}{\rho_G} \cdot \frac{r_0^2(W/B)}{r_0^2(G/L)} \cdot \frac{r_i(W/B)}{r_i(G/L)} \quad (27)$$

For thin annular films

$$\frac{r_i(W/B)}{r_i(G/L)} \doteq \frac{r_0(W/B)}{r_0(G/L)}$$

and Eq. (27) simplifies to

$$\frac{\left(\frac{dP}{dz}\right)_{f(G/L)}}{\left(\frac{dP}{dz}\right)_{f(W/B)}} = \left(\frac{Re_G}{Re_W}\right)^{1.8} \cdot \left(\frac{\mu_G}{\mu_W}\right)^2 \cdot \frac{\rho_W}{\rho_G} \cdot \left[\frac{r_0(W/B)}{r_0(G/L)}\right]^3 \quad (28)$$

The right-hand side of Eq. (28) can be calculated, and the frictional pressure drop in the Earth-based water-benzoate system is to be measured in the laboratory. Hence, the desired frictional pressure drop in the vapor-liquid system in 0-g can be determined.

It is clear from the foregoing analysis that the predicted frictional pressure gradient for zero gravity would depend on the particular correlation used for the dimensionless film thickness and interfacial friction factor. Henstock and Hanratty's[17] analysis was based mainly on results for upward air-water flows in 31.4 mm and 34.5 mm pipes. Hence, its general validity is subject to question. It is for this reason that F is chosen to be the same for the liquid-vapor system in 0-g and for the water-benzoate system in 1-g. If Eqs. (18) and (21) are universally valid, there is no need to use the same F for both systems, thus greatly increasing the flexibility of the simulation scheme.

III. Simulation Experiments

A. Experimental Facility

A simplified schematic of the water-benzoate test facility for simulation of flow in 0-g is shown in Fig. 2. Tap water from a 1.89 m^3 (500 gal) polyethylene storage tank was pumped by a centrifugal pump through 50.8 mm (2 in.) polypropylene pipes into a horizontal test section. The suction head on the centrifugal pump was kept constant by maintaining a fixed water level in the storage tank, which was necessary for maintaining constant flow rate during test runs. The flow rate was controlled by a globe valve located at the pump discharge and monitored by a venturi upstream of the valve. A 25.4 mm (1 inch) venturi was used to monitor water flow rates of up to 6.3×10^{-4} m^{3}s^{-1} (10 gpm). The test section was made of four 19 mm (0.75 in.) o.d. and 15.4 mm i.d. Pyrex glass tubes, each 1.22 m (4 ft) long. They were connected together with standard pipe fittings to form an integral unit approximately 4.88 m (16 ft) in length. The horizontal test section was mounted on a Unistrut superstructure, and metal shims were used to ensure that it was horizontal within close limits. The test section has 14 ports, 0.305 m (12 in.) apart, for mounting pressure probes. Benzoate was injected into the test section using an annular injection nozzle (Fig. 3). It was pumped into the nozzle using a variable-speed gear pump and the flow rate was monitored by variable-area flow meters. The injection

nozzle has three major components: an outer body, an inner tube, and a cap nut. The outer body has four 6.35 mm (0.25 in.) o.d. brass tubes soldered onto it for introducing benzoate. The benzoate flow rates in the four tubes were identical. The upstream end of the outer body has a 1.25 in. NPT male thread for connection to the water feed line. The downstream end of the outer body has a diameter of 19 mm (0.75 in.), which is the same as the outside diameter of the Pyrex test section. It was connected to the inlet end of the Pyrex tube by Swagelok fittings.

The inner tube is fitted into the 15.88 mm (0.625 in.) bore of the outer body. It is 140 mm (5.5 in.) long and has an O-ring seal pressed against the flat face of the counterbore in the outer body. Six recessed guide fins on the outside of the inner tube provided the needed concentricity of the assembly to ensure a uniform annular gap. The cap nut held the inner tube securely in place. The annulus occupies approximately 10% of the total cross-sectional area. The downstream end of the inner tube extended into the pyrex tube to allow visual observation of the interaction between benzoate and water when they first came into contact. The design successfully produced an annular flow with benzoate as the film liquid and water as the core fluid.

Electrically actuated ball valves were provided to direct the mixture flow from the exit of the test section either into the storage tank or into the collection tank for separation and disposal.

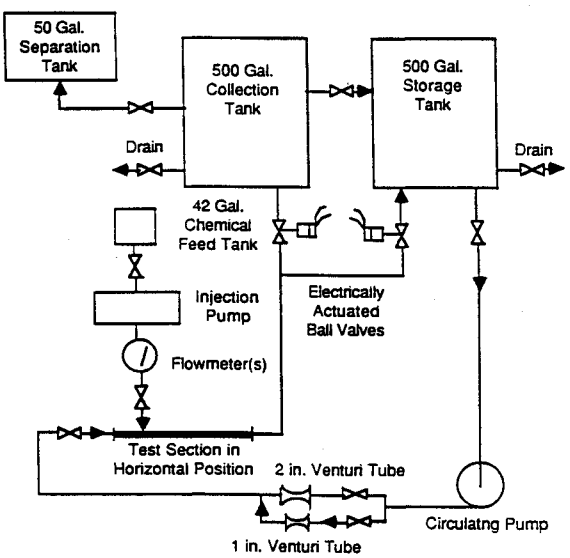

Fig. 2 A simplified schematic of the test facility.

B. Instrumentation

The pressure drop across the 1-in. venturi was measured with a Validyne magnetic reluctance differential pressure transducer. The transducer was calibrated for a range up to 1.4 m (55 in.) of water, corresponding to a maximum flow rate of 0.57 m^3s^{-1} (9.0 gpm), and had an accuracy of 0.25% full scale. The maximum error in the water flow rate measurements was less than 0.6%. The benzoate flow rate in each of the four feeding tubes for the injection nozzle was monitored independently using Omega variable-area flow meters. These flow meters were laboratory calibrated for benzoate flow. The full scale on these meters corresponds to 1.00×10^{-4} m^3s^{-1} (1.58 gpm) and the repeatability is within 0.25% full scale. Another Validyne differential pressure transducer was used to measure the frictional pressure drop across the test section. The transducer was calibrated for a range of 0–920 mm (0–36.2 in.) of water and also had an accuracy of 0.25 percent full scale. The maximum error in the frictional pressure drop measurement was less than 0.7%. The electrical outputs from these transducers were sampled at 25 Hz for a duration of 6 s following the establishment of steady flow.

C. Experimental Procedure

The operational conditions for the water-benzoate experiments were selected in such a way that the measured frictional pressure drop data can be used for simulation schemes based on the Asali et al. correlation,[18] as well as the Henstock and Hanratty correlation.[17] However, the range of operation of the experiments was restricted due to limitations of the available experimental facility and the limited range of flow rates within which the annular flow was stable. It was observed that, for the 15.4 mm i.d. test section, a stable benzoate film could not be maintained when Re_W fell below 18,000. On the other hand, when Re_W exceeded 35,000, the flow appeared emulsified and milky, indicating breakdown of the agitated interfacial wavy surface. For this reason, Re_W was restricted to between 21,000 and 30,000 in the simulation experiments. Outside this range, higher and lower Re_W may be obtained by using test sections of different diameters and/or by using other combinations of neutrally buoyant liquids, but these have not been done in the present study. A requirement for the applicability of Eq. (27) or (28) is that the f_s vs Re_C correlation is the same for the water-benzoate system and for the vapor-liquid system in 0-g. This requirement is met for the range of Re_W just cited.

For reasons already given, the dimensionless parameter F in the Henstock and Hanratty correlation[17] was matched in the simulation experiments. This was accomplished by suitably choosing the flow rates of water and benzoate in such a way that Eq. (25) is satisfied. A detailed illustration of the method, including tabulations of Re_W and Re_B for the simu-

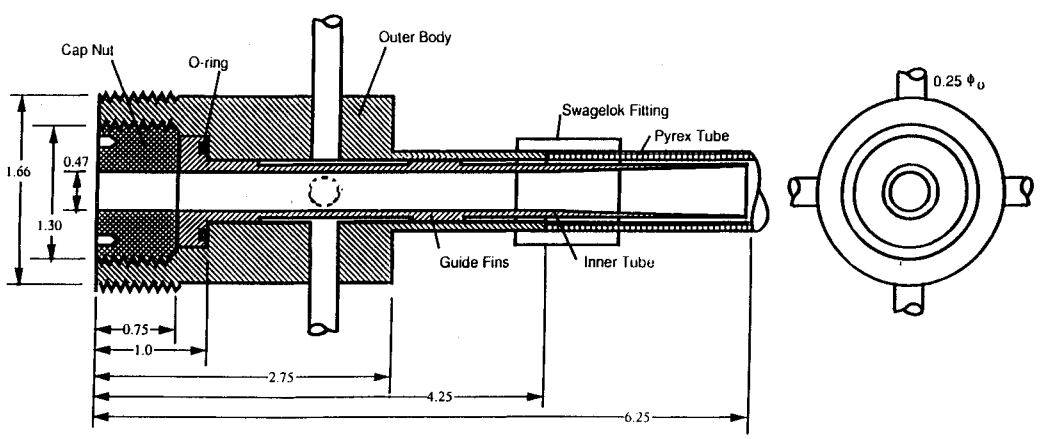

Fig. 3 Injection nozzle for annular flow experiments (dimensions in inches).

lation of refrigerant R11 flow in 0-g, can be found in the appendix to this article. The R11 flow was at a saturation temperature of 290 K in a 12.7 mm i.d. smooth tube. Three mass flow rates, 0.035, 0.042, and 0.065 kgs^{-1}, and five qualities, 0.2, 0.3, 0.4, 0.5, and 0.6, were considered. The water-benzoate simulation experiments were conducted at 286.5 K in the 15.4 mm i.d. test section of the flow facility shown in Fig. 2, using water Reynolds number Re_W = 21,000, 25,500, and 30,000. All pertinent data are given in the Appendix (Tables A1, A2, and A3), including the benzoate Reynolds number Re_B, the water flow rate $\dot{M}_W$, and the benzoate flow rate $\dot{M}_B$. Preliminary runs were performed to ensure that the water-benzoate flow was steady and fully developed in the region of the test section where pressure drop measurements were made.

IV. Results and Discussion

Frictional pressure drop was measured across 1.829 m (6 ft) of the test section where the flow was known to be fully developed. As stated earlier, a Validyne differential pressure transducer with a range of up to 920 mm of water was used for this purpose. It has an accuracy of 0.25% full scale. The data were collected at 25 Hz for a period of 6 s, and two realizations were obtained for each flow condition. The results are presented in Table 1. The values of the pressure drop shown are temporal means. The small differences between the values of $\dot{M}_W$, Re_W, and Re_B shown in Table 1 and their corresponding values listed in the Appendix (Tables A1, A2, and A3) are the result of the minor variations incurred in setting the operational conditions when the simulation experiments were performed.

A. Simulation Scheme Based on Asali et al. Correlation

The theoretical basis of the simulation has been presented in a previous section. The Asali et al. correlations[18] for vertical upflow, Eq. (12), and for vertical downflow, Eq. (14), both show that the ratio f_i/f_s varies directly with $Re_F^{0.6}$. Hence, for horizontal flows and flows in 0-g, it is reasonable to assume that (f_i/f_s) would also vary directly with $Re_F^{0.6}$. Based on this argument, K_4 in Eq. (17) was set to 0.6. The remaining constants K_5 and K_6 in Eq. (17) were evaluated by using a least squares fit for the data presented in Table 1. Using the measured frictional pressure drop, the interfacial shear stress τ_i and then the interfacial friction factor f_i were computed. The connection between f_i and the frictional pressure gradient is prescribed by Eqs. (9) and (10). For the thin annular films that were considered, $r_i \cong r_0$. The correlation parameters K_5 and K_6 determined in this way are 0.00105 and 0.04056, respectively. The mean error of f_i/f_s for this fit is 0.00363 and the standard deviation is 0.01797. The range of f_i/f_s is 1.0014 to 1.2428.

Based on the foregoing results, we obtain the following correlation for the friction factor ratio f_i/f_s for steady, fully developed, annular liquid-vapor flows in 0-g:

$$\frac{f_i}{f_s} - 1 = 0.00105\, Re_F^{0.6}\left(\frac{\mu_F}{\mu_C}\right)\left(\frac{\rho_C}{\rho_F}\right)^{0.5} - 0.04056 \quad (29)$$

where Re_F is defined by Eq. (8a). Equation (29) may be used to determine the frictional pressure drop when the total mass flow rate and vapor quality are given. To illustrate, consideration was given to the prediction of frictional pressure gradient for refrigerant R11 at a saturation temperature of 290

Table 1 Time-averaged frictional pressure drop for water-benzoate annular flow simulating vapor-liquid flow of R11 in 0-g

Water flow rate (kg s^{-1}) $\dot{M}_w$	Re_W[a]	Benzoate flow rate (kg s^{-1}) $\dot{M}_B$	Re_B	Measured pressure drop[b] (mm of water) Mean	SD
0.300	20,930	0.0459	917	477.2	22.8
				485.1	14.4
		0.0214	427	431.7	6.7
				435.6	6.1
		0.0109	218	416.9	5.2
				416.4	5.4
		0.0057	114	406.6	4.7
				407.3	4.3
		0.0029	58	400.9	4.5
				402.4	4.6
0.363	25,305	0.0585	1,168	690.8	16.3
				691.0	15.2
		0.0306	611	620.8	13.3
				620.4	11.6
		0.0145	290	592.4	6.9
				592.6	7.2
		0.0077	154	577.6	6.8
				578.1	6.9
		0.0040	80	559.7	7.4
				559.4	7.8
0.430	29,460	0.0699	1,397	891.6	6.9
				894.1	7.1
		0.0341	682	819.1	18.8
				819.5	17.5
		0.0180	360	765.1	8.8
				765.4	10.0
		0.0097	194	754.2	6.2
				753.8	8.6
		0.0050	99	742.6	7.6
				743.8	7.2

[a]Based on water flow alone in a 15.4 mm i.d. horizontal pipe.
[b]Over a length of 1.829 m in the fully developed region of the test section.

Table 2 Frictional pressure gradient predictions (kPa/m) for R11 flow at 0.035 kg s^{-1} in 12.7 mm i.d. pipe

Vapor quality	Simulation experiment				
	Henstock and Hanratty[17]	Asali et al.[18]	Friedel[24]		
X	0-g	0-g	1-g	0.1-g	0.001-g
0.2	0.626	0.741	3.422	3.123	2.611
0.3	1.170	1.498	4.640	4.262	3.615
0.4	1.887	2.445	5.858	5.419	4.665
0.5	2.754	3.543	7.102	6.615	5.780
0.6	3.774	4.753	8.373	7.853	6.961

Table 3 Frictional pressure gradient predictions (kPa/m) for R11 flow at 0.042 kg s^{-1} in 12.7 mm i.d. pipe

Vapor quality	Simulation experiment				
	Henstock and Hanratty[17]	Asali et al.[18]	Friedel[24]		
X	0-g	0-g	1-g	0.1-g	0.001-g
0.2	0.880	1.068	4.588	4.189	3.504
0.3	1.639	2.155	6.232	5.728	4.862
0.4	2.627	3.509	7.883	7.296	6.288
0.5	3.829	5.073	9.576	8.925	7.808
0.6	5.148	6.785	11.311	10.616	9.423

Table 4 Frictional pressure gradient predictions (kPa/m) for R11 flow at 0.065 kg s^{-1} in 12.7 mm i.d. pipe

Vapor quality	Simulation experiment				
	Henstock and Hanratty[17]	Asali et al.[18]	Friedel[24]		
X	0-g	0-g	1-g	0.1-g	0.001-g
0.2	1.862	2.591	9.264	8.464	7.093
0.3	3.546	5.204	12.640	11.629	9.896
0.4	5.559	8.429	16.064	14.887	12.870
0.5	8.183	12.107	19.604	18.300	16.065
0.6	11.199	16.075	23.266	21.873	19.485

K flowing in a 12.7 mm i.d. smooth pipe at three mass flow rates and five vapor qualities. Table 2 lists the predicted frictional pressure gradient for total mass flow rate of 0.035 kgs^{-1} and vapor qualities of 0.2, 0.3, 0.4, 0.5, and 0.6. Similar data for total mass flow rates of 0.042 and 0.065 kgs^{-1} are listed in Tables 3 and 4. Other entries in these tables will be explained later. These flow rates and vapor qualities were chosen so that the predicted frictional pressure gradient can be directly compared with those based on the Henstock and Hanratty correlation.[17]

B. Simulation Scheme Based on Henstock and Hanratty Correlation[17]

If the simulation scheme using the Henstock and Hanratty correlation[17] with matched F is valid, it must be self-consistent. This was tested in the following way. For a given total mass flow rate and vapor quality of R11 flow in 0-g, several combinations of Re_W and Re_B were chosen based on Eq. (25). Simulation experiments were then conducted using the different combinations of Re_W and Re_B, and the frictional pressure drop over 1.829 m of the test section in the fully developed region was measured. The 0-g frictional pressure drops for the R11 flow calculated from Eq. (27) or (28) using the different combinations of water-benzoate data must agree within experimental error if the scheme is self-consistent. Accordingly, water-benzoate experiments were performed for the simulation of R11 flow in a 12.7 mm i.d. pipe at a total mass flow rate of 0.029 kgs^{-1} and a vapor quality of 30%. Four different values of Re_W were used: 18,960, 21,070, 23,215, and 25,305, each with two realizations. The results are presented in Table 5. The predicted values of the 0-g frictional pressure drops using the four different combinations of Re_W and Re_B were remarkably close, well within 1%. Hence, the simulation scheme is indeed self-consistent. It is recognized that self-consistency is a necessary condition but may not be sufficient. However, time and funding did not permit us to conduct sufficiency tests using test sections of different diameters and neutrally buoyant liquids other than benzoate and water.

Predicted frictional pressure gradients for R11 flow in 0-g at a mass flow rate of 0.035 kgs^{-1} and vapor qualities of 0.2, 0.3, 0.4, 0.5, and 0.6 using the Henstock and Hanratty correlation[17] are compared in Table 2 with those based on the Asali et al. correlation.[18] Tables 3 and 4 contain comparison data for the higher mass flow rates of 0.042 and 0.065 kgs^{-1}. In all instances, predictions based on the Asali et al. correlation[18] are higher. At the present time, it is not possible to speculate on the relative merits of the two schemes. More research is needed.

Table 5 Consistency check of simulation scheme using Henstock and Hanratty correlation (R11 flow at 0.029 kg s^{-1} and vapor quality of 0.3)

Water flow rate (kg s^{-1})	Re_w	Benzoate flow rate (kg s^{-1})	Re_b	Pressure drop: Measured in 1-g W/B flow[a] (mm of water)	Pressure drop: Predicted in 0-g R11 flow[b] (mm of water)
0.272	18,960	0.019	380	365.2	86.2
				366.1	86.4
0.302	21,070	0.022	440	441.5	86.2
				442.3	86.4
0.333	23,215	0.025	500	529.9	86.9
				527.4	86.5
0.363	25,305	0.029	580	616.6	86.6
				614.6	86.3

[a]Over a length of 1.829 m in the fully developed region of a 15.4 mm i.d. test section.
[b]Over a length of 1.829 m in the fully developed region of a 12.7 mm i.d. duct.

C. Comparison of 0-g Frictional Pressure Gradient With Normal and Reduced Gravity Data Based on Friedel Correlation[24]

It is of interest to compare the frictional pressure gradients in dispersed and annular two-phase flows in zero gravity with those under normal gravity at identical mass flow rates and vapor qualities. To this end, we search for a two-phase pressure drop correlation that has been extensively tested. Hewitt wrote in the *Handbook of Multiphase Systems*[23] that recent evaluations based on the Heat Transfer and Fluid Flow Service's propriety data bank have led to the tentative recommendation that the Friedel correlation[24] be used when $\mu_L/\mu_G < 1000$ (which is the case for R11), despite the fact that it is empirical and has no clear physical basis. No statement was made with respect to flow regimes.

Following the examination of 25,000 data points for two-phase frictional pressure drop, Friedel proposed the following equations for horizontal flows and vertical upflows:

$$\phi_{Lo}^2 = E + \frac{3.24\,FH}{(Fr^{0.045})(We^{0.035})} \tag{30}$$

where

$$\phi_{Lo}^2 = \frac{dP_{2\phi,f}/dz}{(dP_f/dz)_{Lo}} \tag{31}$$

$$E = (1 - x)^2 + x^2 \frac{\rho_L f_{Go}}{\rho_G f_{Lo}} \tag{32}$$

$$F = x^{0.78}(1 - x)^{0.24} \tag{33}$$

$$H = \left(\frac{\rho_L}{\rho_G}\right)^{0.91} \left(\frac{\mu_G}{\mu_L}\right)^{0.19} \left(1 - \frac{\mu_G}{\mu_L}\right)^{0.7} \tag{34}$$

$$Fr = \frac{\dot{m}^2}{gD\rho_{TP}^2} \tag{35}$$

$$We = \frac{\dot{m}^2 D}{\rho_{TP}\sigma} \tag{36}$$

$$\rho_{TP} = \left(\frac{x}{\rho_G} + \frac{1 - x}{\rho_L}\right)^{-1} \tag{37}$$

in which ϕ_{Lo}^2 is the two-phase frictional multiplier, $dP_{2\phi,f}/dz$ is the two-phase frictional pressure gradient, $(dP_f/dz)_{Lo}$ is the single-phase frictional pressure gradient at the same total mass flux and with the same liquid properties, x is the vapor quality, $\dot{m}$ is the total mass flux, and D is the hydraulic diameter. All properties are designated by the usual notation. The single-phase friction factors f_{Go} and f_{Lo} are calculated using the Blasius equation:

$$f = 0.079\left(\frac{\dot{m}D}{\mu}\right)^{-0.25} \tag{38}$$

where μ implies μ_L or μ_G as the case may be.

Friedel's correlation[24] is based on data collected under Earth gravity and, hence, it is questionable if it can be used for reduced or zero gravity. Nevertheless, an exercise has been performed to predict the frictional pressure gradient in 0.1-g and 0.001-g, in addition to 1-g. The frictional pressure gradients are determined for fully developed dispersed and annular flows of R11 in a 12.7 mm i.d. pipe at total mass flow rates of 0.035, 0.042, and 0.065 kg s^{-1}. The frictional pressure gradients for dispersed flows are calculated for vapor qualities of up to 0.2%. The 0-g frictional pressure drops for the latter conditions are computed using a scheme developed by the authors.[1] This scheme states that the frictional pressure drop in fully developed, dispersed, liquid-vapor flow in straight ducts of constant cross section at 0-g is identical to that due to liquid flowing alone at the same total volumetric flow rate of the liquid-vapor mixture. The frictional pressure drops for the *dispersed* flow regimes in 0-g and in normal and reduced gravity are plotted in Figs. 4a, 5a, and 6a for total mass flow rates of 0.035, 0.042, and 0.065 kg s^{-1}, respectively. The frictional pressure gradients for the *annular* flows are computed for vapor qualities ranging from 20%–60%. Figures 4b, 5b, and 6b compare the normal and reduced gravity results with the 0-g predictions based on the Asali et al.[18] and Henstock and Hanratty[17] simulation schemes. The data used in plotting these figures are listed in Tables 2, 3, and 4. All normal and reduced gravity data, *dispersed* and *annular*, were calculated from the Friedel correlation.[24]

The foregoing results demonstrate that frictional pressure gradients in 0-g, either in the dispersed or annular flow regime, are lower than those in 1-g for identical mass flux and quality. This finding contradicts that concluded by Chen et al.[6] Chen et al. reported pressure drop data for the flow of saturated R114 in a horizontal duct of 15.8 mm i.d. with contiguous straight and curved test sections at mass fluxes ranging from 192 to 228 kg m^{-2}s^{-1} (flow rates: 0.038 to 0.045 kg s^{-1}) and vapor qualities ranging from 5%–90%. Pressure drops were measured across the straight section, the curved section, and the entire test section in Earth gravity and in microgravity created aboard a NASA KC-135 aircraft flying parabolic trajectories. They reported that the frictional pressure drop in microgravity was *higher* than that at 1-g and that the greatest percentage increase was in the low quality region. The data that are relevant to the present work are those measured in 1-g and in microgravity across the straight sec-

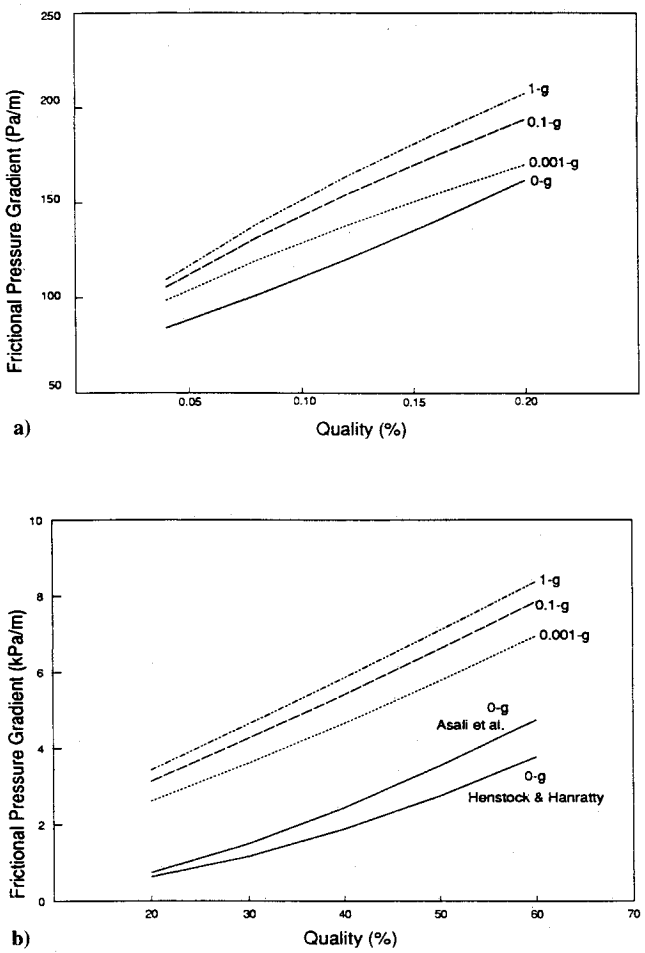

Fig. 4 Comparison of the frictional pressure gradient predictions with Friedel correlation[24] for R11 annular flows in a 12.7 mm duct at 0.035 kg s^{-1}: a) dispersed flow regime and b) annular flow regime.

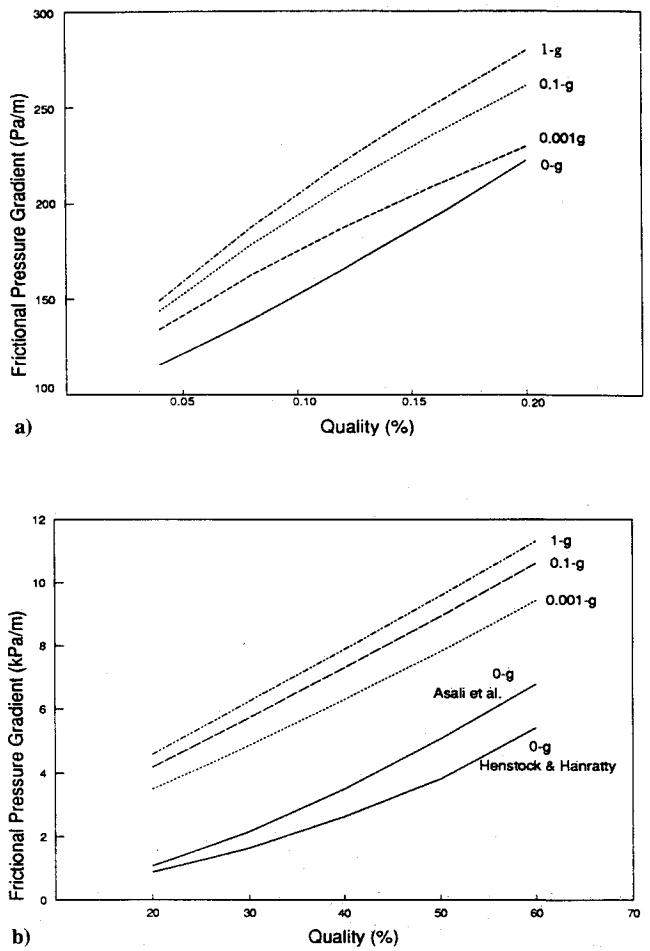

Fig. 5 Comparison of the frictional pressure gradient predictions with Friedel correlation[24] for R11 annular flows in a 12.7 mm duct at 0.042 kg s^{-1}: a) dispersed flow regime and b) annular flow regime.

tion, 1.83 m in length. The measurements were made by Sunstrand Energy Systems,[25] who reported that the uncertainty in the frictional pressure drop measurements was ±344 Pa (±0.05 psi) which, in a number of cases, is greater than or comparable to the measured values. Accordingly, conclusions based on these measurements are suspect.

Flow fluctuations and oscillations have been observed in two-phase flow experiments conducted aboard NASA KC-135 aircraft during the microgravity part of the flight created by the fore and aft accelerations of the aircraft flying parabolic trajectories.[26] The effect of such unsteadiness on the microgravity pressure drop measurements has not been investigated. The use of contiguous straight and curved test sections creates complexities undesirable for the proper interpretation of data. While Chen et al.[6] reported observing classical annular flows for vapor qualities ranging from 0.2 to 0.6 under microgravity conditions, stratified flow was observed under 1-*g* for vapor qualities ranging from 0.2 to 0.41, and stratified semi-annular flow for vapor qualities ranging from 0.54 to 0.62. Hence, the two-phase data studied by Chen et al. in microgravity and in 1-*g* might not be in the same flow regime.

The present prediction schemes reveal that the frictional pressure drop in both dispersed and annular flows is lower in 0-*g* than in 1-*g* under otherwise identical conditions. That this is so may be explained from the physics of the flows. In dispersed liquid-vapor flows in 0-*g*, it has been shown that the mean dispersed phase velocity is equal to the local mean continuous phase velocity.[1] In 1-*g* flows, the vapor bubble would have a velocity different from that of its surrounding liquid, resulting in extraneous dissipation of energy and, hence, a higher frictional pressure drop. For horizontal annular flows in 1-*g*, both entrainment and nonuniformity of the film thickness along the circumference of the duct would result in a higher frictional pressure drop. In 0-*g*, liquid droplets entrained in the vapor core are expected to travel at the same velocity as the vapor that surrounds them—a simple but important fact unearthed in our investigation of dispersed flows.[1] In 1-*g* the droplets would be lagging behind the vapor, causing energy dissipation. The liquid film thickness of horizontal annular flows in 1-*g* varies along the circumference of the duct. It is thinner in the upper portion of the duct and thicker in the lower portion. Fisher and Pearce[27] measured the circumferential film thickness for various pipe diameters and superficial velocities. They found that in a 12 mm i.d. tube at superficial air and water velocities of 22.4 ms^{-1} and 0.9 ms^{-1}, respectively, the film thickness was 0.3 mm at the top of the tube and 0.8 mm at the bottom. The average thickness for the nonuniform film is smaller than that for uniform film at the same mass flow rate of the film fluid. The average interfacial shear stress is greater for the nonuniform film. Considering this fact alone, the frictional pressure drop should be greater in 1-*g* than at 0-*g*.

Friedel's correlation[24] has been recommended for horizontal and vertical upflows. For vertical upflows, the average annular film thickness would be expected to be uniform, and the effect due to entrainment in 0-*g* and in 1-*g* is similar to that just discussed for horizontal flows. However, there exists another effect in vertical flows; it tends to increase the pressure drop in 1-*g*, but not in 0-*g*. This is the buoyancy effect, which would increase the relative velocity between the vapor

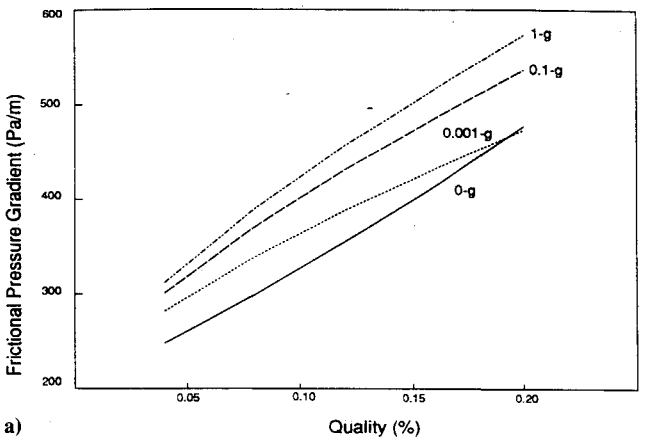

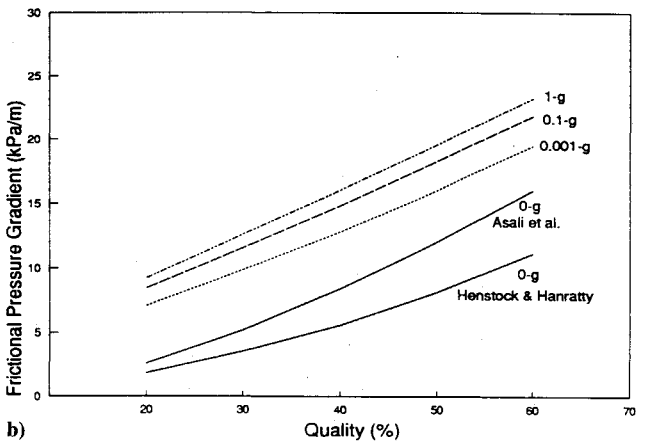

Fig. 6 Comparison of the frictional pressure gradient predictions with Friedel correlation[24] for R11 annular flows in a 12.7 mm duct at 0.065 kg s^{-1}: a) dispersed flow regime and b) annular flow regime.

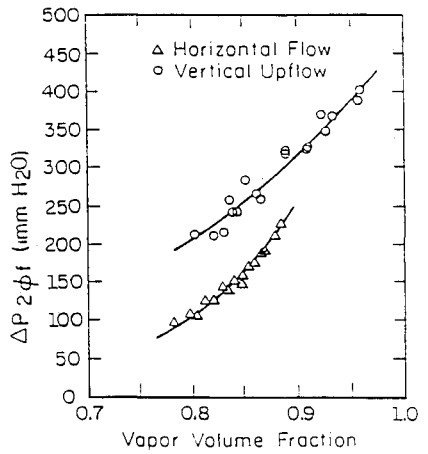

Fig. 7 Frictional pressure drop for vertical upflow and horizontal flow of saturated R11 in an adiabatic section (G = 401 kgm^{-2} s^{-1}).[22]

and the liquid. The higher velocity difference would not only increase the interfacial shear stress but also enhance entrainment.

Klausner[22] measured frictional pressure drops in 1-g in vertical upflows and horizontal flows of R11 in a 19.1 mm tube over a wide range of mass fluxes. While annular flows were observed for vertical upflows at high volume fractions of the vapor, stratified semi-annular flows were observed for horizontal flows. At a given mass flow rate, the tendency toward annular flow was greater at higher vapor qualities. His adiabatic frictional pressure drop data for horizontal and vertical upward flows at a mass flux of 401 kgm^{-2}s^{-1} are reproduced in Figure 7. It is seen that frictional pressure drop is consistently lower in horizontal flow, where gravity exerts a smaller influence than in vertical flows.

Appendix

The dimensionless flow parameter F introduced by Henstock and Hanratty[17] to characterize the roughness of the interface in annular flows was defined by Eq. (18). In the simulation scheme used, F was matched for both the water-benzoate (1-g) and liquid-vapor (0-g) systems. This matching was achieved by satisfying Eq. (25).

To illustrate, consider the flow of refrigerant R11 in 0-g at a saturation temperature of 290 K in a 12.7 mm i.d. smooth tube. The relevant properties are

$$\rho_L = 1.495 \text{ kgm}^{-3} \qquad \rho_G = 4.639 \text{ kgm}^{-3}$$

$$\mu_L = 454 \times 10^{-6} \text{ Pa·s} \qquad \mu_G = 10.63 \times 10^{-6} \text{ Pa·s}$$

The simulation experiments were performed in a 15.4 mm i.d. smooth tube at 286.5 K. Thus, the relevant properties are

$$\rho_B = 1{,}000 \text{ kgm}^{-3} \qquad \rho_W = 999.3 \text{ kgm}^{-3}$$

$$\mu_B = 4.14 \times 10^{-3} \text{ Pa·s} \qquad \mu_W = 1.185 \times 10^{-3} \text{ Pa·s}$$

Accordingly, the dimensionless group on the right-hand side of Eq. (25) has the value

$$\frac{\mu_L}{\mu_G}\frac{\mu_W}{\mu_B}\left(\frac{\rho_W}{\rho_L}\right)^{0.5} = 0.681$$

For a given total mass flow rate of R11 and a specified vapor quality, x, the mass flow rates of liquid, $\dot{M}_L$, and its vapor $\dot{M}_G$, are known. Hence, Re_G and Re_L can be determined. For a suitable value of Re_W, the corresponding Re_B can be calculated from Eq. (25). The water and benzoate flow rates corresponding to R11 flows of 0.035, 0.042, and 0.065 kg s^{-1} and vapor qualities of 20–60% are tabulated in Tables A1 through A3.

Acknowledgments

This research was supported by NASA Kennedy Space Center under contract NAS10-11153. Thanks are due to F. N. Lin of KSC for his many helpful discussions and to Thad-

Table A1 Flow conditions for simulation of 0-g liquid-vapor flow of R11 at a mass flow rate of 0.035 kg s^{-1}

X	$\dot{M}_G$ (kg s^{-1})	$\dot{M}_L$ (kg s^{-1})	Re_G	Re_L	Re_W	Re_B	$\dot{M}_B$ (kg s^{-1})	$\dot{M}_W$ (kg s^{-1})
0.2	0.0070	0.0280	66,019	6,183	21,000	917	0.0459	0.3010
0.3	0.0105	0.0245	99,029	5,410	21,000	426	0.0213	0.3010
0.4	0.0140	0.0210	132,039	4,637	21,000	217	0.0109	0.3010
0.5	0.0175	0.0175	165,048	3,864	21,000	114	0.0057	0.3010
0.6	0.0210	0.0140	198,058	3,092	21,000	60	0.0030	0.3010

$2r_0$ = 12.7 for R11 and 15.4 mm for water-benzoate systems

Table A2 Flow conditions for simulation of 0-*g* liquid-vapor flow of R11 at a mass flow rate of 0.042 kg s^{-1}

X	$\dot{M}_G$ (kg s^{-1})	$\dot{M}_L$ (kg s^{-1})	Re_G	Re_L	Re_W	Re_B	$\dot{M}_B$ (kg s^{-1})	$\dot{M}_W$ (kg s^{-1})
0.2	0.0084	0.0336	79,223	7,420	25,500	1,170	0.0586	0.3655
0.3	0.0126	0.0294	118,835	6,492	25,500	557	0.0279	0.3655
0.4	0.0168	0.0252	158,447	5,565	25,500	289	0.0145	0.3655
0.5	0.0210	0.0210	198,058	4,637	25,500	153	0.0077	0.3655
0.6	0.0252	0.0168	237,670	3,710	25,500	80	0.0040	0.3655

$2r_0$ = 12.7 for R11 and 15.4 mm for water-benzoate systems

Table A3 Flow conditions for simulation of 0-*g* liquid-vapor flow of R11 at a mass flow rate of 0.065 kg s^{-1}

X	$\dot{M}_G$ (kg s^{-1})	$\dot{M}_L$ (kg s^{-1})	Re_G	Re_L	Re_W	Re_B	$\dot{M}_B$ (kg s^{-1})	$\dot{M}_W$ (kg s^{-1})
0.2	0.0130	0.0520	122,607	11,483	30,000	1,398	0.0700	0.4300
0.3	0.0195	0.0455	183,911	10,048	30,000	675	0.0338	0.4300
0.4	0.0260	0.0390	245,215	8,612	30,000	353	0.0177	0.4300
0.5	0.0325	0.0325	306,519	7,177	30,000	188	0.0094	0.4300
0.6	0.0390	0.0260	367,822	5,741	30,000	98	0.0049	0.4300

$2r_0$ = 12.7 for R11 and 15.4 mm for water-benzoate systems

deus Niezyniecki for his assistance in conducting the simulation experiments.

References

[1]Sridhar, K. R., Chao, B. T., and Soo, S. L., "Pressure Drop in Fully Developed Duct Flow of Dispersed Liquid-Vapor Mixtures at Zero-Gravity," *Acta Astronautica*, Vol. 21, No. 9, 1990, pp. 617–627.

[2]Sridhar, K. R., "Pressure Drop in Fully Developed, Turbulent, Liquid-Vapor Duct Flows at Zero Gravity," Ph.D. Dissertation, Univ. of Illinois at Urbana-Champaign, IL, 1990.

[3]Lovell, T. W., "Liquid-Vapor Flow Regime Transitions for Use in Design of Heat Transfer Loops in Spacecraft—An Investigation of Two-Phase Flow in Zero Gravity Conditions," Air Force Wright Aeronautical Laboratories TR-85-3021, Wright-Patterson AFB, OH, 1985.

[4]Reddy-Karri, S. B., and Mathur, V. K., "Two-Phase Flow Regime Map Predictions Under Microgravity," *AIChE Journal*, Vol. 34, No. 1, 1988, pp. 137–139.

[5]Dukler, A. E., Fabre, J. A., McQuillen, J. B., and Vernon, R., "Gas-Liquid Flow at Microgravity Conditions: Flow Patterns and Their Transitions," *International Symposium on Thermal Problems in Space-Based Systems*, ASME HTD-Vol. 83, 1987, pp. 85–97.

[6]Chen, I.-Y., Downing, R. S., Parish, R., and Keshock, E., "A Reduced Gravity Flight Experiment: Observed Flow Regimes and Pressure Drops of Vapor and Liquid Flow in Adiabatic Piping," *AIChE Symposium* Series 263, Vol. 84, 1988, pp. 203–216.

[7]Calvert, S., and Williams, B., "Upward Co-Current Annular Flow of Air and Water in Smooth Tubes," *AIChE Journal*, Vol. 1, No. 1, 1955, pp. 78–86.

[8]Charvonia, D. A., "A Study of the Mean Thickness of the Liquid Film and the Characteristics of the Interfacial Surface in Annular Two-Phase Flow in a Vertical Pipe," Jet Propulsion Center Report I-59-I, Purdue Univ. and Purdue Research Foundation, West Lafayette, IN, 1959.

[9]Anderson, G. H., and Mantzouranis, B. G., "Two-Phase (Gas-Liquid) Flow Phenomena: I, Pressure Drop and Hold-Up for Two-Phase Flow in Vertical Tubes," *Chemical Engineering Science/Journal International de Genie Chimique*, Vol. 12, No. 2, 1960, pp. 109–126.

[10]Roberts, D. C., and Hartley, D. E., "A Correlation of Pressure Drop Path for Two-Phase Annular Flows in Vertical Channels," Nuclear Research Memorandum Q6, Queen Mary College, London, 1961.

[11]Gill, L. E., Hewitt, G. F., Hitchon, J. W., and Lacey, P. M. C., "Sampling Probe Studies of the Gas Core in Annular Two-Phase Flow: I, The Effect of Length on Phase and Velocity Distribution," *Chemical Engineering Science/Journal International de Genie Chimique*, Vol. 18, No. 8, 1963, pp. 525–535.

[12]Hewitt, G. F., and Lacey, P. M. C., "The Breakdown of the Liquid Film in Annular Two-Phase Flow," *International Journal of Heat and Mass Transfer*, Vol. 8, No. 5, 1965, pp. 781–791.

[13]Shearer, C. J., and Nedderman, R. M., "Pressure Gradient and Film Thickness in a Co-Current Upwards Flow of Gas-Liquid Mixtures: Application to a Film-Cooler Design," *Chemical Engineering Science/Journal International de Genie Chemique*, Vol. 20, No. 7, 1968, pp. 671–683.

[14]Levy, S., "Prediction of Two-Phase Critical Flow-Rate," *Journal of Heat Transfer*, Series C, Vol. 87, No. 1, 1965, pp. 53–58.

[15]Wallis, G. B., "Vertical Annular Flow: I, A Simple Theory; II, Additional Effect," Annual Meeting of the AIChE, Tampa, FL, May 1968.

[16]Hewitt, G. F., and Hall-Taylor, N. S., *Annular Two-Phase Flow*, Pergamon Press, Elmsford, NY, 1970.

[17]Henstock, W. H., and Hanratty, T. J., "The Interfacial Drag and the Height of the Wall Layer in Annular Flows," *AIChE Journal*, Vol. 22, No. 6, 1976, pp. 990–1000.

[18]Asali, J. C., Hanratty, T. J., and Andreussi, P., 1985, "Interfacial Drag and Film Height for Vertical Annular Flow," *AIChE Journal*, Vol. 31, No. 6, 1985, pp. 895–902.

[19]Cousins, L. B., Denton, W. H., and Hewitt, G. F., "Liquid Mass Transfer in Annular Two-Phase Flow," Atomic Energy Research Establishment Rept. R4926, 1965.

[20]Andreussi, P., and Zanelli, S., "Downward Annular and Annular-Mist Flow of Air-Water Mixtures," *Two-Phase Momentum, Heat and Mass Transfer in Chemical, Process, and Energy Engineering Systems*, Vol. 1, Hemisphere, New York, 1979, pp. 303–314.

[21]Webb, D., "Studies of the Characteristics of Downward Annular Two-Phase Flow; 3. Measurements of Entrainment Rate, Pressure Gradient, Probability Distribution on Film Thickness and Disturbance Wave Inception," Atomic Energy Research Establishment Rept. R6426, 1970.

[22]Klausner, J. F., "The Influence of Gravity on Pressure Drop and Heat Transfer in Flow Boiling," Ph.D. Dissertation, Univ. of Illinois at Urbana-Champaign, IL, 1989.

[23]Hewitt, G. F., "Pressure Drop (in Liquid-Gas Systems)," *Handbook of Multiphase Systems*, edited by G. Hetsroni, Hemisphere, New York, 1982, Chap. 2.

[24]Friedel, L., "Improved Pressure Drop Correlations for Horizontal and Vertical Two-Phase Pipe Flow," Paper E3, European Two-Phase Flow Group Meeting, Ispra, Italy, 1979.

[25]Sunstrand Energy Systems, "A Study of Two-Phase Flow in a Reduced Gravity Environment," Final Report, Sunstrand Corp., Rockford, IL, 1987.

[26]Kachnik, L., Lee, D., Best, E., and Faget, N., "A Microgravity Boiling and Convective Condensation Experiment," American Society of Mechanical Engineers Paper 87-WA/HT112, 1987.

[27]Fischer, S. A., and Pearce, D. L., "A Theoretical Model for Describing Annular Flows," *Two-Phase Momentum, Heat and Mass Transfer in Chemical, Process, and Energy Engineering Systems*, Vol. 1, Hemisphere, New York, 1979, pp. 327–337.